Delay in hepatocyte proliferation and prostaglandin D2 synthase expression for cholestasis due to endotoxin during partial hepatectomy in rats

YUSUKE WAKASA[1], NORIHISA KIMURA[1], TOSHIYUKI YAMADA[2], TAKESHI SHIMIZU[2], KENICHI HAKAMADA[1] and SHIGEKI TSUCHIDA[2,3]

Departments of [1]Gastroenterological Surgery and [2]Biochemistry and Genome Biology, Hirosaki University Graduate School of Medicine, Hirosaki, Aomori 036-8562; [3]Department of Rehabilitation Sciences, Hirosaki University of Health and Welfare, Hirosaki, Aomori 036-8102, Japan

Received February 19, 2019; Accepted August 22, 2019

DOI: 10.3892/mmr.2019.10681

Abstract. Infection is a frequent complication of liver transplantation or partial hepatectomy (PH) and sometimes results in cholestasis. We examined factors involved in infection-induced cholestasis after PH, employing a rat PH model and lipopolysaccharide (LPS) as a bacterial toxin. Male Sprague-Dawley rats were subjected to 70% PH and/or LPS injection, and tissues were harvested at 0, 24, 72 and 168 h. Gene expression was analyzed by microarray analysis and reverse transcription-quantitative polymerase chain reaction, and protein levels and localization were analyzed by western blotting and immunohistochemistry, respectively. Plasma bile acid levels were significantly higher in the LPS + PH group than in the PH group. Ribonucleotide reductase regulatory subunit M2 and proliferating cell nuclear antigen peaked at 24 and 72 h in the PH group and LPS + PH group, respectively, indicating a delay in cell proliferation in the latter group. The sodium-dependent taurocholate cotransporting polypeptide and organic-anion-transporting polypeptide 1a1 and 1a2 were reduced in the PH group at 24 h, and were not further decreased in the LPS + PH group. Chemokine ligand 9 (Cxcl9), a chemokine involved in M2 macrophage polarization, increased after 24 h in the LPS and the LPS + PH groups. The number and shape of Cxcl9-positive cells were similar to CD163-positive cells, suggesting that such cells produced the chemokine. Hematopoietic prostaglandin D_2 synthase (Ptgds2) was only detected in hepatocytes of the LPS + PH group exhibiting a delay in cell proliferation. Thus, Kupffer cells activated with LPS were suggested to be responsible for a delay in hepatocyte proliferation after PH.

Correspondence to: Professor Shigeki Tsuchida, Department of Rehabilitation Sciences, Hirosaki University of Health and Welfare, 3-18-1 Sanpinai, Hirosaki, Aomori 036-8102, Japan
E-mail: tsuchidas@jyoto-gakuen.ac.jp

Key words: cholestasis, partial hepatectomy, lipopolysaccharide, ABC transporter, liver regeneration, Kupffer cell, chemokine

Introduction

The liver is a unique organ with the capacity to regenerate following the removal of two-thirds of liver mass (1). Liver regeneration requires the precisely coordinated proliferation of the two major hepatic cell populations, hepatocytes and liver sinusoidal endothelial cells to reconstitute liver structure and function (2). Liver regeneration also requires the interaction between hepatocytes and other component cells, such as Kupffer cells and hepatic stellate cells (1,3,4). Numerous molecules, including hepatocyte growth factor and epidermal growth factor have been demonstrated as mitogens produced in nonparenchymal cells (5). Suppressed liver regeneration is of major concern for small remnant liver volume in adult living donor transplantation or in bacterial infection after partial hepatectomy (PH), as this has been associated with cholestasis and mortality (6).

Hepatocytes under physiological conditions efficiently extract bile acids from sinusoids via the sodium-dependent taurocholate cotransporting polypeptide (Ntcp) and the sodium-independent organic anion transporting polypeptide (Oatp1) (7). The extracted bile acids are excreted into the bile canaliculi by ATP-dependent transporters, such as the bile salt export pump (7). In our previous study, 90% PH in rats resulted in high blood bile acids levels and the suppression of Ntcp expression (6). Thus, lower uptake of bile acids has been suggested to be partly involved in cholestasis (6).

Infection is a frequent complication after living donor liver transplantation (8). Low-dose lipopolysaccharide (LPS) application after PH in mice was reported to delay liver proliferation (9). As LPS is known to activate Kupffer cells (10), this suggests that activated Kupffer cells may inhibit liver proliferation; however, it has been demonstrated that Kupffer cells stimulate liver regeneration after PH (1); depletion of Kupffer cells by clodronate delays liver regeneration (11). Therefore, Kupffer cells activated by LPS may lose their capacity to induce hepatocyte proliferation after PH.

The present study examined whether LPS-induced cholestasis is also due to the suppression of Ntcp expression, as observed in 90% PH rats. It also examined whether Kupffer cells activated by LPS inhibit or stimulate liver regeneration after PH. The expression of anion transporters for the uptake from the sinusoid was decreased in PH, but LPS did not further decrease their expression. This suggested that decreases in these transporters were not responsible, but a delay in hepatocyte proliferation may be linked to LPS-induced cholestasis. LPS treatment alone or in combination with PH induced Kupffer cell activation with a CD163-positive phenotype, a marker for M2-type macrophages (12); CD163-positive cells were suggested to produce chemokine ligand 9 (Cxcl9), which was determined to be involved in chronic inflammation (13) and M2 macrophage polarization (14). As hematopoietic type prostaglandin D2 synthetase (Ptgds2) is known to inhibit lymphocyte proliferation (15), Ptgds2 staining was performed. Hepatocytes in the LPS + PH group were stained and markedly stained at 24 h, a time point when cell proliferation was notably inhibited. On the contrary, hepatocytes in the LPS or the PH groups were not stained.

Materials and methods

Animals and animal treatment. Male Sprague-Dawley rats weighing 180-220 g and 6 weeks old were purchased from Charles River Laboratories Japan, Inc. In total 39 rats were used and they were housed under routine laboratory conditions at the animal laboratory of Hirosaki University. The rats received standard laboratory chow, had free access to food and water, and were kept in a thermostatically controlled room (25˚C) with a 12-h light-dark cycle. Before undergoing surgical procedures, all rats were fasted for 24 h. The rats were divided into five groups: Control group without any treatment, sham group receiving laparotomy alone, LPS group receiving intravenous LPS 75 μg/rat, PH group receiving 70% PH, and LPS + PH group receiving intravenous LPS injection immediately after PH. 70% PH was performed as reported previously (6). The rats of four groups except the control group were sacrificed at 24, 72 and 168 h after laparotomy or PH and/or LPS treatment. Those of the control group were sacrificed at 0 h. Three rats each were used at respective time points of each group. LPS (O55:B5, L2880) was purchased from Sigma-Aldrich (Merck KGaA). After the surgical procedures, the rats had free access to a 200 g/l glucose solution for 24 h to avoid post-operative hypoglycemia after hepatectomy. The present study was performed in accordance with the Guidelines for Animal Experimentation, Hirosaki University, and all of the animals received humane care according to the criteria outlined in the 'Guide For The Care And Use Of Laboratory Animals' prepared by the National Academy of Sciences and published by the National Institutes of Health (16).

Plasma total bilirubin and bile acids. Blood from the hearts was collected in test tubes containing EDTA and plasma was prepared after centrifugation at 2,500 x g, for 10 min at room temperature. Plasma total bilirubin, aspartate aminotransferase (AST), and alanine aminotransferase (ALT) were measured using Spotchem EZ (ARKRAY, Inc.) with SPOTCHEM II Basic Panel 2 Test Strips (MT-7785; ARKRAY, Inc.), according to the manufacturer's protocols. The plasma levels of total bile acids were measured with an assay kit (Diazyme Laboratories), according to the manufacturer's protocol.

Microarray analysis. Total RNA was extracted from frozen liver samples at 0, 24, 72 and 168 h after 70% hepatectomy and/or LPS injection with TRIzol® reagent (Thermo Fisher Scientific, Inc.). Equal amounts of RNA from three individual livers were combined, and 10 μg of RNA was used to produce biotin-labeled complementary RNA (cRNA) with GeneChip IVT labeling kit (Affymetrix; Thermo Fisher Scientific, Inc.). The labeled and fragmented cRNA was subsequently hybridized to GeneChip® Rat Gene-ST 2.0 Array (Affymetrix; Thermo Fisher Scientific, Inc.). Labeling, hybridization, image scanning and data analysis were performed at TOHOKU CHEMICAL Co., Ltd.

Reverse transcription-quantitative polymerase chain reaction (RT-qPCR). Complementary DNA (cDNA) was reverse-transcribed from 1 μg of total RNA using the Omniscript RT kit (Qiagen, Inc.), according to the manufacturer's protocols. A MiniOpticon Detection System (Bio-Rad Laboratories, Inc.) and SYBR® Green Supermix (Bio-Rad Laboratories, Inc.) were used for the quantitation of specific mRNA. The amplification of *ubiquitin C* cDNA was performed to standardize the levels of the target cDNA, as reported previously (6). Gene-specific primers were designed according to known rat sequences (Table I). PCR amplification consisted of 30 sec at 94˚C, 30 sec at 55-60˚C and 30 sec at 72˚C for 30-35 cycles. No non-specific PCR products, as detected by melting temperature curves, were found. After normalizing the expression of the target gene to *ubiquitin C* expression using the $2^{-\Delta\Delta Ct}$ method reported by Livak and Schmittgen (17) in triplicate; the levels of mRNA expression in three samples at respective time points (0, 24, 72, and 168 h after treatment) were expressed relative to the control values.

Western blotting. Crude liver membranes were prepared according to the method of Gant *et al* (18) and the samples (100 μg protein each) were dissolved in sample buffer and separated via 7.5% SDS-PAGE with a 4.4% stacking gel. Protein content was measured by Bradford's method (19) using a bovine serum albumin standard curve. Following electrophoresis, the proteins were transferred to polyvinylidene fluoride membranes (Hybond-P, GE Healthcare). After blocking with 4% nonfat dry milk in Tris-buffered saline for 2 h at room temperature, membranes were incubated overnight at 4˚C with primary anti-Ntcp antibody (sc-107029; 1:10,000, Santa Cruz Biotechnology, Inc.) or anti-β-actin antibody (ab227387; 1:1,000, Abcam). Immune complexes were detected using a horseradish peroxidase conjugated anti-rabbit IgG secondary antibody (NA934; 1:2,000, GE Healthcare) and visualized with an enhanced chemiluminescent kit (ECL Plus; GE Healthcare).

Immunostaining. Liver tissue samples were fixed in 10% neutral buffered formaldehyde for two days at 4˚C and embedded in paraffin. These paraffin blocks were sliced into 4 μm sections and passed through xylene and a graded alcohol series. The

Table I. Reverse transcription-quantitative polymerase chain reaction primer sequences.

Gene	Forward primer (5'→3')	Reverse primer (5'→3')
Abcc2	CACAGGTTTGCCCATTATCC	ATATTGAGGGCGTTGGACAG
Slc10a1	AGGCATGATCATCACCTTCC	AAGTGGCCCAATGACTTCAG
Slc21a1	TACATGTCAGCTTGCCTTGC	GCGGGAATACCAGCAAATAC
Slc21a2	CAATTCGGTATCCCCACATC	GTTTGAGGACACGTTGCTTG
Rrm2	GCACTGGGAAGCTCTGAAAC	GGCAATTTGGAAGCCATAGA
Pcna	GGTGAAGTTTTCTGCGAGTG	CTCAGAAGCGATCGTCAAAG
Cxcl9	TCGAGGAACCCTAGTGATAAGGAATCAG	TTTGCTTTTTCTTTTGGCTGATCTTTTTC

Abcc2, ATP binding cassette subfamily C member 2; Slc10a1, sodium-dependent taurocholate cotransporting polypeptide; Slc21a1, solute carrier organic anion transporter 1a1; Slc21a2, solute carrier organic anion transporters 1a2; Rrm2, ribonucleotide reductase regulatory subunit M2; Pcna, proliferating cell nuclear antigen; Cxcl9, chemokine ligand 9.

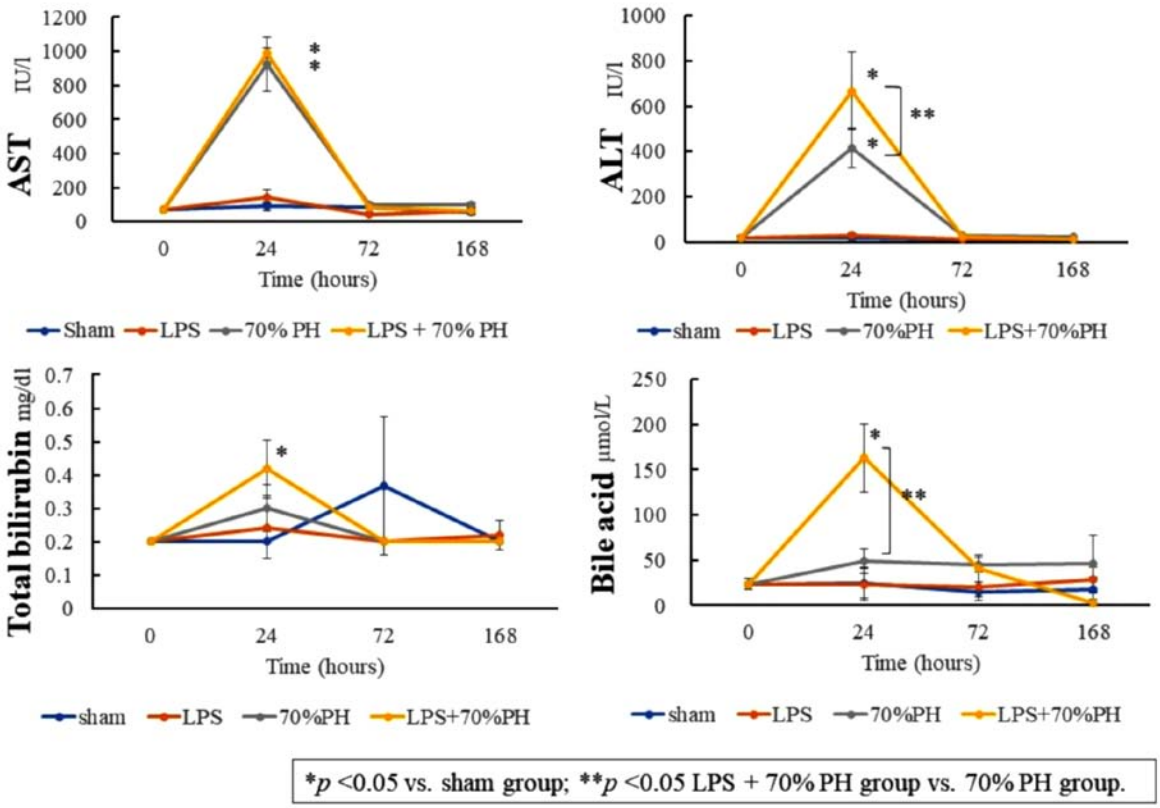

Figure 1. Levels of plasma AST, ALT, total bilirubin and bile acids at 0 (control), 24, 72, and 168 h after a sham operation (blue), LPS administration (orange), 70% PH (gray), and LPS + 70% PH (yellow). The biomarker levels were quantified with a commercial kit. Data are presented as the mean ± standard deviation from three rats. *P<0.05 vs. sham group; **P<0.05 LPS + 70% PH group vs. 70% PH group. ALT, alanine aminotransferase; AST, aspartate aminotransferase; LPS, lipopolysaccharide; PH, partial hepatectomy.

deparaffinized sections were stained with hematoxylin solution at room temperature for 5 min. Following washing with water and passing through a graded alcohol series, the sections were stained with eosin solution for 1 min. The deparaffinized sections were also stained for CD68, CD163, Cxcl9, and Ptgds2 using a standard avidin-biotin-peroxidase conjugate method (20) using an automated immunostaining instrument (Benchmark XT; Ventana Medical System). The slides were blocked with 0.3% hydrogen peroxide and then incubated for 1 h at room temperature with the primary antibodies. The antibodies employed were: Anti-CD68 antibody (MCA 341R; 1:100, Bio-Rad Laboratories, Inc.), anti-CD 163 antibody (sc-58965; 1:500, Santa Cruz Biotechnology, Inc.), anti-Cxcl9 antibody (bs-2551R; 1:500, BIOSS Inc.), and anti-Ptgds2 antibody (PA 5-43217; 1:500, Invitrogen; Thermo Fisher Scientific, Inc.). Non-immune γ-globulin fractionated from rabbit sera by 20-40% saturation of ammonium sulfate (21) was used as a negative control instead of primary antibody. The biotinylated anti-rabbit IgG or anti-mouse IgG antibodies and Vectastain ABC kit (PK6101) were obtained from Vector

Table II. Results of microarray analysis.

Cellular function and gene name (*gene symbol*)	Signal											
		Sham			LPS			70% PH			LPS + 70% PH		
	Control (0 h)	24 h	72 h	168 h	24 h	72 h	168 h	24 h	72 h	168 h	24 h	72 h	168 h
DNA replication													
Ribonucleotide reductase subunit M2 (*Rrm2*)	450	40	30	70	70	420	120	2,290[a]	660	270	470	860	40
Topoisomerase (DNA)II α (*Top2a*)	250	30	40	70	70	190	70	750[a]	260	120	190	390	30
Proliferating cell nuclear antigen (*Pcna*)	240	120	160	130	170	200	130	540[a]	250	170	240	300	190
DNA ligase I (*Lig1*)	60	30	40	60	50	70	60	120[a]	80	50	60	110	40
Kupffer cells													
Cd68 molecule (*Cd68*)	240	280	240	260	260	230	210	170	300	360	260	300	450
Cd163 molecule (*Cd163*)	260	320	250	260	200	270	250	230	310	350	270	300	380
Mannose receptor, C type 1 (*Mrc1*)	450	550	440	490	420	580	490	400	510	520	370	570	570
Chemokine (C-X-C motif) ligand 1 (*Cxcl1*)	50	110	120	70	120	50	60	470[a]	250[a]	230[a]	260[a]	210[a]	270[a]
Chemokine (C-X-C motif) ligand 9 (*Cxcl9*)	120	80	80	140	4,770[a]	280[a]	130	100	160	140	4,140[a]	310[a]	110
Chemokine (C-X-C motif) receptor 3 (*Cxcr3*)	40	30	40	40	30	30	30	30	40	20	30	30	40
Stellate cells													
Collagen, typeI, α1 (*Col1a1*)	110	90	470	120	130	190	160	110	250	210	150	350	220
Desmin (*Des*)	50	40	60	50	60	60	40	50	60	50	60	60	60
Liver progenitor cells													
Cytokeratin 19 (*Krt19*)	30	40	50	30	20	40	40	30	30	210	30	30	30
Epithelial cell adhesion molecule (*Epcam*)	80	80	100	70	90	80	90	50	70	50	60	70	90
Sinusoid transporter													
ATP binding cassette subfamily C member 1 (*Abcc1*)	20	30	30	30	30	30	30	40	30	30	30	40	30
ATP binding cassette subfamily C member 3 (*Abcc3*)	110	150	220	100	130	110	70	70	140	70	90	200	90
Solute carrier family 10 member 1 (*Slc10a1*, Ntcp)	3,650	3,620	2,880	3,170	2,850	3,490	3,370	1,090[b]	3,090	3,370	740[b]	3,120	3,320
Solute carrier organic anion transporter family, member 1a1 (*Slc21a1*, Oatp1)	1,170	1,150	840	830	680	880	850	530[b]	610	850	380[b]	770	770
Solute carrier organic anion transporter family, member 1a2 (*Slc21a2*, Oatp2)	950	480	520	570	220[b]	1,060	730	140[b]	820	730	90[b]	900	320
Bile canaliculus transporter													
ATP binding cassette subfamily C member 2 (*Abcc2*)	1,870	1,510	1,880	30	1,510	2,570	2,910	1,030	1,860	2,910	760[b]	2,000	2,690
ATP binding cassette subfamily B member 11 (*Abcb11*)	2,190	2,260	2,030	100	1,610	2,260	2,450	1,630	2,310	2,450	1,470	2,260	2,480
ATP binding cassette subfamily G member 5 (*Abcg5*)	340	240	260	3,170	190	290	190	100[b]	120[b]	190	130[b]	160[b]	80[b]
ATP binding cassette subfamily G member 8 (*Abcg8*)	170	100	110	830	70	110	70	50[b]	50[b]	70	70[b]	60[b]	40[b]
ATP binding cassette subfamily B member 1A (*Abcb1a*)	140	130	140	570	110	140	100	60	130	100	80	170	80
ATP binding cassette subfamily B (MDR/TAP) member 1B (*Abcb1b*)	140	30	180	30	60	130	40	820[a]	280[a]	40	160	500[a]	60
ATP binding cassette subfamily B member 4 (Abcb4)	670	750	620	100	880	680	650	710	950	650	1,030	940	530

[a]More than 2-fold higher signal than those in the control or sham groups. [b]Less than half the signal than those in the control or sham groups. LPS, lipopolysaccharide; PH, partial hepatectomy.

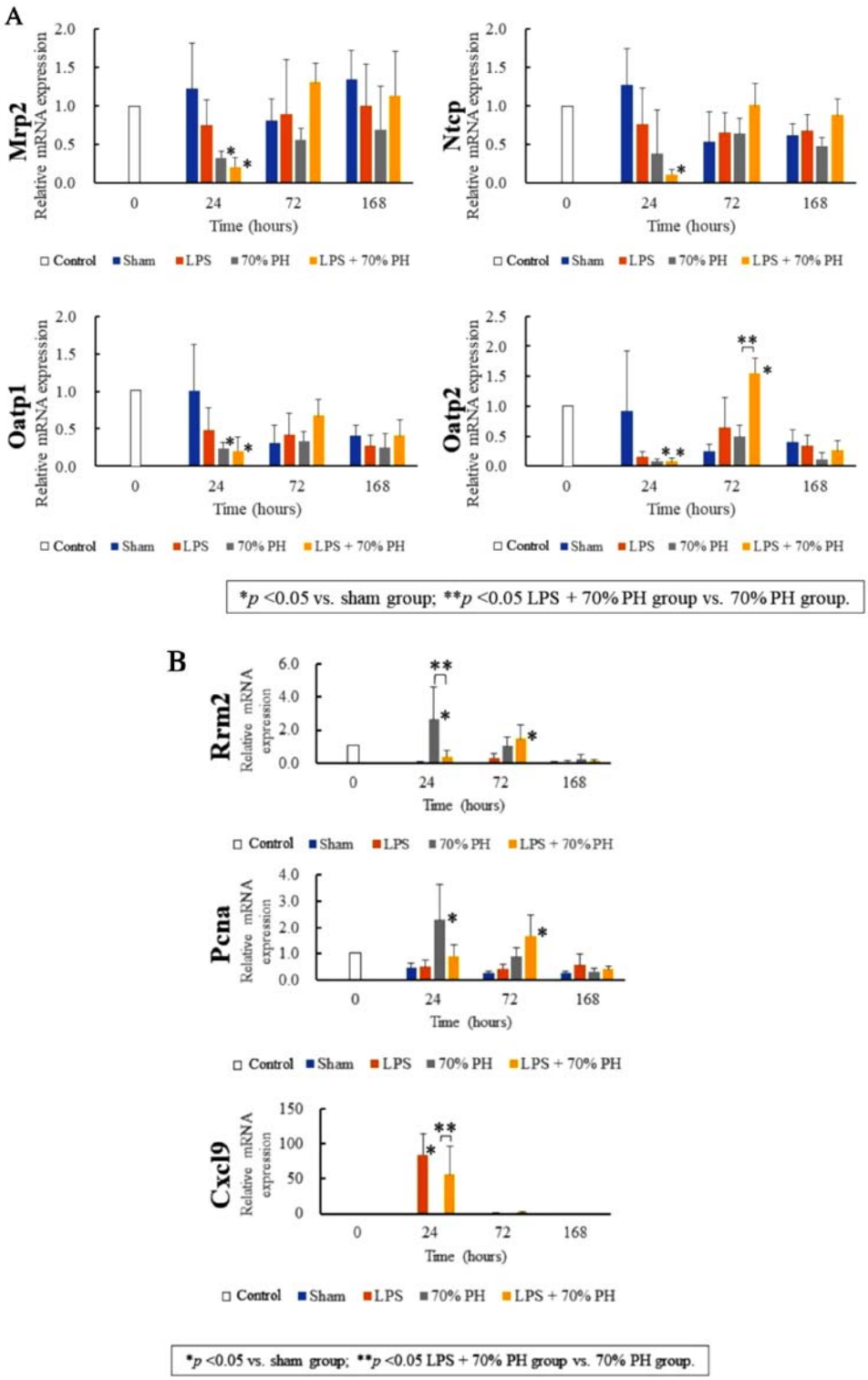

Figure 2. Quantitation of mRNA expression. The expression of (A) organic anion transporters, and (B) DNA replication genes and Cxcl9 at 0, 24, 72, and 168 h after the sham operation (blue), LPS administration (orange), PH (gray), and LPS + PH (yellow). The quantification of *Mrp2*, *Ntcp*, *Oatp1*, *Oatp2*, *Rrm2*, *Pcna* and *Cxcl9* mRNA expression was conducted via reverse transcription-quantitative polymerase chain reaction. The mRNA expression levels at 24, 72 and 168 h are expressed relative to the values of individual mRNA at 0 h. Data are presented as the mean ± standard deviation from three rats. *P<0.05 vs. sham group; **P<0.05 LPS + 70% PH group vs. 70% PH group. Mrp2, ATP binding cassette subfamily C member 2; Ntcp, taurocholate cotransporting polypeptide; Oatp1, solute carrier organic anion transporters 1a1; Oatp2, solute carrier organic anion transporters 1a2; Rrm2, ribonucleotide reductase regulatory subunit M2; Pcna, proliferating cell nuclear antigen; Cxcl9, chemokine ligand 9; LPS, lipopolysaccharide; PH, partial hepatectomy.

Laboratories, Inc. The specific binding was visualized with a 3,3'-diaminobenzidine tetrahydrochloride solution. Sections were then lightly counterstained with hematoxylin for microscopic examination. Images were captured with an inverted FSX 100 microscope (Olympus Corporation). Digital images were processed with Adobe Photoshop (version 7.0, Adobe Systems, Inc.) and ImageJ software (v1.50, National Institutes of Health).

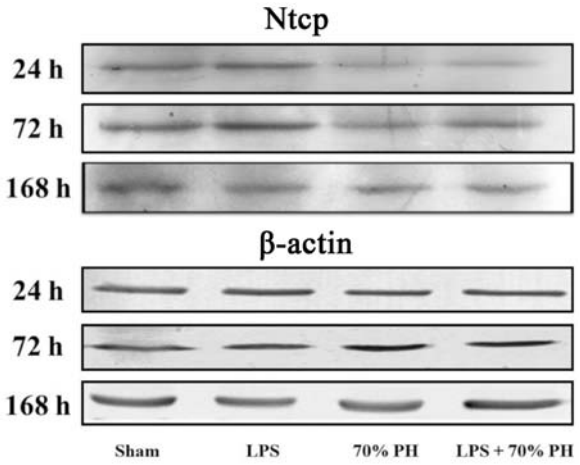

Figure 3. Western blotting for Ntcp in liver tissue membrane samples at 24, 72, and 168 h after each operation, and for β-actin; 100 μg of protein was separated per lane. Ntcp, taurocholate cotransporting polypeptide; LPS, lipopolysaccharide; PH, partial hepatectomy.

Statistical analysis. Experiments for which a statistical analysis was indicated were performed independently at least three times. Data are presented as the mean ± standard deviation. Statistical comparisons were analyzed using SPSS software (v22.0, IBM Corp.). Differences between experimental groups were assessed for significance using two-way ANOVA with a Tukey's post-hoc test. $P<0.05$ was considered to indicate a statistically significant difference.

Results

Elevated plasma bilirubin and bile acid levels in the LPS + PH group. Bilirubin and bile acid levels in the plasma at 24 h post-operation were significantly increased in the LPS + PH group compared with those in the sham group. The bile acid level was significantly higher in the LPS + PH group than that in the PH group (Fig. 1). These results indicated that LPS induced cholestasis in this rat model. AST and ALT levels in the plasma at 24 h were significantly increased in the LPS + PH group and PH group, compared with those in the sham group.

Suppression and delay in DNA replication in the LPS + PH group. Microarray analysis was performed to comprehensively analyze alterations in liver gene expression. Data were expressed as signal values, and changes of >2-fold or <1/2 from the values in the control or sham groups were considered significant. Ribonucleotide reductase regulatory subunit M2 (*Rrm2*), DNA topoisomerase IIα and proliferating cell nuclear antigen (*Pcna*), which are markers of DNA replication (6), reached a peak level of expression after 24 h in the PH group and gradually decreased thereafter. However, in the LPS + PH group, these replication signals were low after 24 h and peaked after 72 h. The values at 72 h were lower than those at 24 h in the PH group (Table II). These results suggested a delay and suppression in DNA replication in the LPS + PH group. No notable changes were observed in *Cd68* or *Cd163* expression, which are markers of Kupffer cells (12,22). The chemokine *Cxcl9* markedly increased in the LPS group and LPS +PH group, compared with that in the sham at 24 h (Table II). For sinusoid transporters, Ntcp (*Slc10a1*), Oatp1(*Slc21a1*) and Oatp2 (*Slc21a2*) were reduced in the LPS + PH and the PH groups at 24 h. These expression levels returned to control levels at 72 h in both groups. No notable changes were observed in collagen 1α1 or desmin, markers of hepatic stellate cells, or in cytokeratin19 or epithelial cell adhesion molecule, markers of liver progenitor cells (23) (Table II).

To confirm these changes in gene expression, RT-qPCR was performed. *Abcc2*, *Oatp1*, and *Oatp2* mRNA levels were significantly decreased at 24 h in the LPS + PH group and PH group, compared with those in the sham group. These mRNA levels except *Oatp2* were not significantly different between the LPS + PH and the PH groups (Fig. 2A). The *Rrm2* mRNA levels at 24 h in the LPS + PH group were lower than those in the PH group (Fig. 2B). *Rrm2* and *Pcna* peaked at 24 h in the PH group, whereas at 72 h, the levels increased in the LPS + PH group (Fig. 2B), confirming the results obtained by microarray analysis. *Cxcl9* showed a significant rise after 24 h in the LPS and LPS + PH groups compared with the control and PH groups, respectively (Fig. 2B). These findings suggested that *Cxcl9* expression was dependent on LPS treatment.

Ntcp protein levels were examined by western blotting; Ntcp expression was decreased in the PH and LPS + PH group at 24 h compared with the sham group (Fig. 3).

Expression of Cxcl9 in Kupffer cells activated by LPS treatment. Although *Cd68* mRNA or *Cd163* mRNA levels were unaltered as determined by microarray analysis (Table II), staining for CD68, a marker of Kupffer cells and macrophages (22), revealed a marked increase in CD68-positive Kupffer cells in the LPS and LPS + PH groups, compared with that in the sham and PH groups (Fig. 4A). CD163 staining, a marker for M2 macrophages and Kupffer cells (12) was positive in cells in the LPS and LPS + PH groups (Fig. 4B). These CD163-positive cells were not detected in the sham or PH groups. There were fewer CD163-positive cells than CD68-positive cells, and their cell shapes were different from each other. These results suggested that CD163-positive cells detected after LPS treatment denoted M2-type Kupffer cells (12). There were also Cxcl9-positive cells in the LPS and LPS + PH groups (Fig. 4C), whereas Cxcl9-positive cells were not detected in the sham or PH groups. The number of Cxcl9-positive cells was similar to that of CD163-positive cells rather than CD68-positive cells (Fig. 4D).

Expression of Ptgds2 in hepatocytes in the LPS + PH group. As Ptgds2 inhibits cell proliferation (15), Ptgds2 staining was performed. A positive reaction was only detected in hepatocytes of the LPS + PH group, but not in other groups (Fig. 5). Kupffer cells were not stained in any groups. In the LPS + PH group, Ptgds2 was markedly stained in hepatocytes at 24 h, weakly stained at 72 h, but not at 168 h.

Discussion

In the rat PH model of the present study, LPS treatment induced cholestasis and delayed cell proliferation. Compared with the sham group, the expression of anion transporters involved in the uptake from the sinusoid was downregulated at 24 h in both the PH and the LPS + PH groups, but did not differ between the

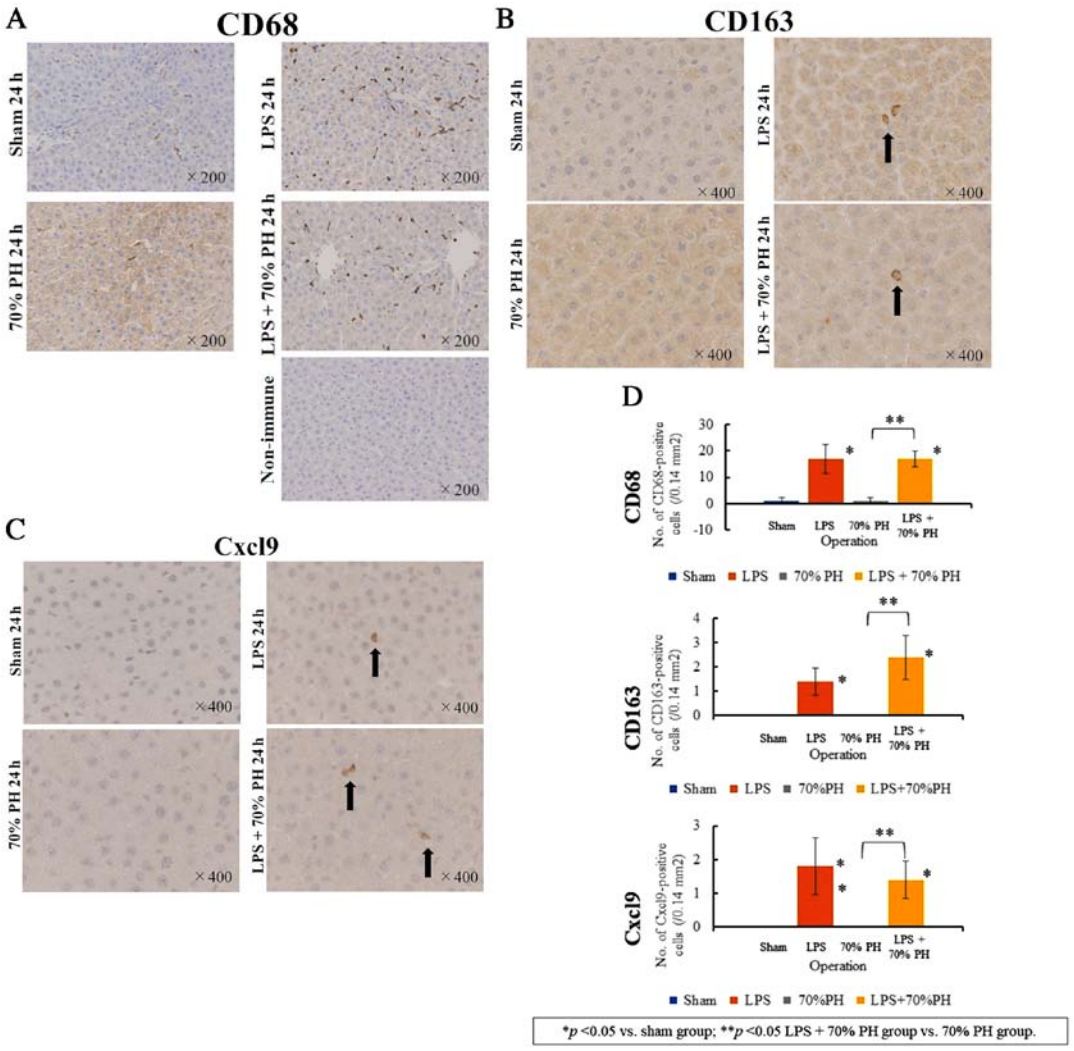

Figure 4. Immunostaining. (A) CD68, (B) CD163, and (C) Cxcl9 expression in the sham, LPS, PH and LPS + PH groups at 24 h. Staining was also analyzed with non-immune γ-globulin for (A). Arrows in the panels indicated positive cells. The data presented are from a representative preparation set and are similar to the results obtained from other sets. Original magnification: (A) x200, and (B and C) x400. (D) Number of CD68-, CD163- and Cxcl9-positive cells. The cells in the liver sections were from five microscope fields (0.14 mm^2) from each rat. Data are presented as the mean ± standard deviation from three rats. *P<0.05 vs. sham group; **P<0.05 LPS + PH group vs. PH group. LPS, lipopolysaccharide; PH, partial hepatectomy.

latter two groups. Downregulation of these anion transporters is a causative factor for cholestasis after 90% PH (6,7,24). However, this was unlikely in the case of cholestasis in the LPS + PH group; suppression or delays in cell proliferation may be the responsible factor. Downregulation of marker genes of DNA replication, such as *Rrm2* was determined by RT-qPCR analysis; however, delays in cell proliferation are not confirmed by protein levels, as immunohistochemistry for Pcna was not conducted. Hepatocyte proliferation is blocked by 2-acetylaminofluorene administration during PH in rats (25). In this case, biliary epithelial cells and hepatic stellate cells become progenitor cells, and these cells contribute to liver regeneration (25). In the case of LPS, activation of these cells was not detected, and microarray and RT-qPCR data suggested that hepatocyte proliferation was inhibited transiently.

Our findings revealed that LPS treatment increased the count of CD68-positive cells and CD163-positive cells. These results confirmed the activation of Kupffer cells by LPS as reported previously (26). From microarray analysis, *Cd68* and *Cd163* expression was determined to be unaffected by

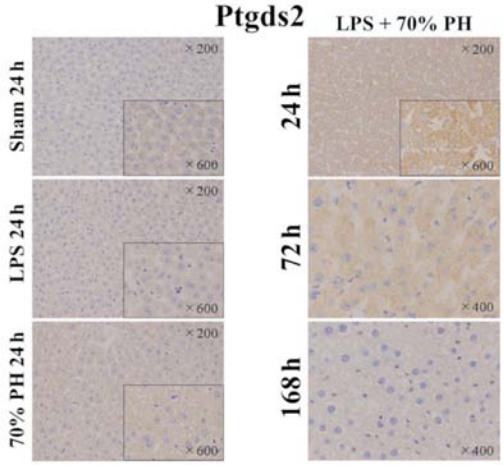

Figure 5. Immunostaining for hematopoietic Ptgds2 in the sham, LPS, PH and LPS + PH groups at 24 h. Original magnification: x200; the small panels are of a higher magnification (magnification, x600) of the original panel. Immunostaining for Ptgds2 in LPS + PH group on 72, and 168 h (original magnification, x400). Ptgds2, prostaglandin D_2 synthase; LPS, lipopolysaccharide; PH, partial hepatectomy.

LPS treatment despite increases in the number of CD68- and CD163-positive cells as detected by immunostaining. This discrepancy may reflect a difference between mRNA and protein expression; however, further investigation is required. As CD163 is a marker of M2-type macrophages (12,22), CD163-positive cells may belong to M2-Kupffer cells (22). Thus, CD68-positive cells may denote M1-type macrophages or Kupffer cells (27). A marked increase in the number of CD68-positive cells by LPS treatment raises two possibilities: The proliferation of CD68-positive cells in the liver or the migration of CD68-positive cells to the liver from bone marrow (28,29). The absence of alterations in *Cd68* mRNA levels by LPS treatment suggests the latter explanation as a more likely possibility.

In the present study, *Cxcl9* was significantly induced by LPS treatment. Immunohistochemistry suggested that Cxcl9 was expressed by CD163-positive cells. Double staining for Cxcl9 and CD163 should be conducted to establish this possibility. Cxcl9 is a member of a family of ligands for the Cxcr3 receptor, which is involved in chronic inflammation and cancer (13). Cxcl9 is also a biomarker of acute cellular rejection after liver transplantation (30). Endothelial cell growth is stimulated or inhibited depending on alternatively spliced variants of Cxcr3 (31). Cxcl9 is expressed in macrophages (32,33) and C-X-C motif chemokine receptor 3 (Cxcr3) promotes M2 macrophage polarization in human liver cancer (14). Prostaglandin E_2 inhibits CXCR3 ligand secretion induced by interferon-γ treatment in human breast cancer cells (34).

Ptgds2 is the hematopoietic-type Ptgds and is expressed in mast cells and macrophages (35). Ptgds2 is also expressed in skeletal muscle cells with muscular dystrophy (36). Inhibition of Ptgds2 stimulates the survival of muscle cells via the suppression of muscular cell death (37). Lymphocytes isolated from Ptgds2 knock-out mice exhibit hyperproliferation (15). The time courses of Ptgds2 staining and cell proliferation had opposite profiles in our study. Thus, Ptgds2 was suggested to suppress hepatocyte proliferation. Ptgds2 was not detected in the LPS or PH groups, but was expressed in hepatocytes of the LPS + PH group. These results indicated that LPS and cell proliferation signals may be required for the induction of Ptgds2 expression in hepatocytes. The findings indicating that LPS alone did not alter cell proliferation suggested that a delay in cell proliferation in the LPS + PH group may not be due to the direct effects of LPS on hepatocytes, but due to Kupffer cells activated by LPS. Cxcl9 may be a candidate signaling molecule released from Kupffer cells for Ptgds2 expression in hepatocytes; however, because Cxcl9 was produced by LPS alone, Cxcl9 may not be sufficient for Ptgds2 expression. Ptgds2 may be a target to prevent a delay in cell proliferation after PH induced by LPS or bacterial infections.

Acknowledgements

The authors would like to thank Ms. Yukie Fujita and Ms. Sayumi Kubo (Department of Pathology and Bioscience, Hirosaki University Graduate School of Medicine) for their technical assistance in immunostaining, and Ms. Ryoko Seito, Mr. Hitoshi Kudo and Ms. Ikumi Shirahama (Institute for Animal Experimentation, Hirosaki University Graduate School of Medicine) for their technical assistance for animal treatment.

Funding

The present study was partly supported by the Japan Society for the Promotion of Science KAKENHI (grant no. 15K20845; Grant-in-Aid for Young Scientists B). No additional external funding was received for this study.

Availability of data and materials

All data generated or analyzed during the present study are included in this published article.

Authors' contributions

YW, NK and ST conceived the idea and design of the present study. YW, NK, TY and TS performed the animal experiments. YW, KH and ST wrote the manuscript. YW, NK and ST discussed the results and contributed to the final version of the manuscript. KH performed the statistical analyses. All authors approved the final version of the manuscript to be published.

Ethics approval and consent to participate

All animal experiments were conducted strictly according to ethical standards and approved by the Animal Ethical Committee of Hirosaki University Graduate School of Medicine (approval ID: M15041).

Patient consent for publication

Not applicable.

Competing interests

The authors declare that they have no competing interests.

References

1. Preziosi ME and Monga SP: Update on the mechanisms of liver regeneration. Semin Liver Dis 37: 141-151, 2017.
2. Hu J, Srivastava K, Wieland M, Runge A, Mogler C, Besemfelder E, Terhardt D, Vogel MJ, Cao L, Korn C, *et al*: Endothelial cell-derived angiopoietin-2 controls liver regeneration as a spatiotemporal rheostat. Science 343: 416-419, 2014.
3. Marrone G, Shah VH and Bracia-Sancho J: Sinusoidal communication in liver fibrosis and regeneration. J Hepatol 65: 608-617, 2016.
4. Mabuchi A, Mullaney I, Sheard PW, Hessian PA, Mallard BL, Tawadrous MN, Zimmermann A, Senoo H and Wheatley AM: Role of hepatic stellate cell/hepatocyte interaction and activation of hepatic stellate cells in the early phase of liver regeneration in the rat. J Hepatol 40: 910-916, 2004.
5. DeLeve LD: Liver sinusoidal endothelial cells and liver regeneration. J Clin Invest 123: 1861-1866, 2013.
6. Miura T, Kimura N, Yamada T, Shimizu T, Nanashima N, Yamana D, Hakamada K and Tsuchida S: Sustained repression and translocation of Ntcp and expression of Mrp4 for cholestasis after rat 90% partial hepatectomy. J Hepatol 55: 407-414, 2011.
7. Cuperus FJ, Claudel T, Gautherot J, Halilbasic E and Trauner M: The role of canalicular ABC transporters in cholestasis. Drug Metab Dispos 42: 546-560, 2014.
8. Abad CL, Lahr BD and Razonable RR: Epidemiology and risk factors for infection after living donor liver transplantation. Liver Transpl 23: 465-477, 2017.

9. Jörger AK, Liu L, Fehlner K, Weisser T, Cheng Z, Lu M, Höchst B, Bolzer A, Wang B, Hartmann D, *et al*: Impact of NKT cells and LFA-1 on liver regeneration under subseptic conditions. PLoS One 11: e0168001, 2016.
10. Liu H, Liao R, He K, Zhu X, Li P and Gong J: The SMAC mimetic birinapant attenuates lipopolysaccharide-induced liver injury by inhibiting the tumor necrosis factor receptor-associated factor 3 degradation in Kupffer cells. Immunol Lett 185: 79-83, 2017.
11. Meijer C, Wiezer MJ, Diehl AM, Schouten HJ, Schouten HJ, Meijer S, van Rooijen N, van Lambalgen AA, Dijkstra CD and van Leeuwen PA: Kupffer cell depletion by Cl2MDP-liposomes alters hepatic cytokine expression and delays liver regeneration after partial hepatectomy. Liver 20: 66-77, 2000.
12. Edin S, Wikberg ML, Dahlin AM, Rutegard J, Oberg A, Oldenborg PA and Palmqvist R: The distribution of macrophages with a M1 or M2 phenotype in relation to prognosis and the molecular characteristics of colorectal cancer. PLoS One 7: e47045, 2012.
13. Billottet C, Quemener C and Bikfalvi A: CXCR3, a double-edged sword in tumor progression and angiogenesis. Biochim Biophys Acta 1836: 287-295, 2013.
14. Liu RX, Wei Y, Zeng QH, Chan KW, Xiao X, Zhao XY, Chen MM, Ouyang FZ, Chen DP, Zheng L, *et al*: Chemokine (C-X-C motif) receptor 3-positive B cells link interleukin-17 inflammation to protumorigenic macrophage polarization in human hepatocellular carcinoma. Hepatology 62: 1779-1790, 2015.
15. Trivedi SG, Newson J, Rajakariar R, Jacques TS, Hannon R, Kanaoka Y, Eguchi N, Colville-Nash P and Gilroy DW: Essential role for hematopoietic prostaglandin D2 synthase in the control of delayed type hypersensitivity. Proc Natl Acad Sci USA 103: 5179-5184, 2006.
16. National Research Council (US) Committee for the Update of the Guide for the Care and Use of Laboratory Animals: Guide for the Care and Use of Laboratory Animals. 8th edition, National Academies Press, Washington, DC, 2011.
17. Livak KJ and Schmittgen TD: Analysis of relative gene expression data using real-time quantitative PCR and the 2(-Delta Delta C(T)) method. Methods 25: 402-408, 2001.
18. Gant TW, Silverman JA, Bisgaard HC, Burt RK, Marino PA and Thorgeirsson SS: Regulation of 2-acetylaminofluorene- and 3-methylcholanthrene-mediated induction of multidrug resistance and cytochrome P450IA gene family expression in primary hepatocyte cultures and rat liver. Mol Carcinog 4: 499-509, 1991.
19. Bradford MM: A rapid and sensitive method for the quantitation of microgram quantities of protein utilizing the principle of protein-dye binding. Anal Biochem 72: 248-254, 1976.
20. Hsu SM, Raine L and Fanger H: Use of avidin-biotin-peroxidase complex (ABC) in immunoperoxidase techniques: A comparison between ABC and unlabeled antibody (PAP) procedures. J Histochem Cytochem 29: 577-580, 1981.
21. Hebert GA: Ammonium sulfate fractionation of sera: Mouse, hamster, guinea pig, monkey, chimpanzee, swine, chicken, and cattle. Appl Microbiol 27: 389-393, 1974.
22. Dixon LJ, Barnes M, Tang H, Pritchard MT and Nagy LE: Kupffer cells in the liver. Compr Physiol 3: 785-797, 2013.
23. Yovchev MI, Grozdanov PN, Zhou H, Racherla H, Guha C and Dabeva MD: Identification of adult hepatic progenitor cells capable of repopulating injured rat liver. Hepatology 47: 636-647, 2008.
24. Chang TH, Hakamada K, Toyoki Y, Tsuchida S and Sasaki M: Expression of MRP2 and MRP3 during liver regeneration after 90% partial hepatectomy in rats. Transplantation 77: 22-27, 2004.
25. Kordes C, Sawitza I, Götze S, Herebian D and Häussinger D: Hepatic stellate cells contribute to progenitor cells and liver regeneration. J Clin Invest 124: 5503-5515, 2014.
26. Suzuki S, Nakamura S, Serizawa A, Sakaguchi T, Konno H, Muro H, Kosugi I and Baba S: Role of Kupffer cells and the spleen in modulation of endotoxin-induced liver injury after partial hepatectomy. Hepatology 24: 219-225, 1996.
27. Tacke F and Zimmermann HW: Macrophage heterogeneity in liver injury and fibrosis. J Hepatol 60: 1090-1096, 2014.
28. Aldeguer X, Debonera F, Shaked A, Krasinkas AM, Gelman AE, Que X, Zamir GA, Hiroyasu S, Kovalovich KK, Taub R and Olthoff KM: Interleukin-6 from intrahepatic cells of bone marrow origin is required for normal murine liver regeneration. Hepatology 35: 40-48, 2002.
29. Nishiyama K, Nakashima H, Ikarashi M, Kinoshita M, Nakashima M, Aosasa S, Seki S and Yamamoto J: Mouse CD11b+Kupffer cells recruited from bone marrow accelerate liver regeneration after partial hepatectomy. PLoS One 10: e0136774, 2015.
30. Asaoka T, Marubashi S, Kobayashi S, Hama N, Eguchi H, Takeda Y, Tanemura M, Wada H, Takemasa I, Takahashi H, *et al*: Intragraft transcriptome level of CXCL9 as biomarker of acute cellular rejection after liver transplantation. J Surg Res 178: 1003-1014, 2012.
31. Lasagni L, Francalanci M, Annunziato F, Lazzeri E, Giannini S, Cosmi L, Sagrinati C, Mazzinghi B, Orlando C, Maggi E, *et al*: An alternatively spliced variant of CXCR3 mediates the inhibition of endothelial cell growth induced by IP-10, Mig, and I-TAC, and acts as functional receptor for platelet factor 4. J Exp Med 197: 1537-1549, 2003.
32. Farber JM: A macrophage mRNA selectively induced by gamma-interferon encodes a member of the platelet factor 4 family of cytokines. Proc Natl Acad Sci USA 87: 5238-5242, 1990.
33. Metzemaekers M, Vanheule V, Janssens R, Struyf S and Proost P: Overview of the mechanisms that may contribute to the non-redundant activities of interferon-inducible CXC chemokine receptor 3 ligands. Front Immunol 8: 1970, 2018.
34. Bronger H, Kraeft S, Schwarz-Boeger U, Cerny C, Stöckel A, Avril S, Kiechle M and Schmitt M: Modulation of CXCR3 ligand secretion by prostaglandin E2 and cyclooxygenase inhibitors in human breast cancer. Breast Cancer Res 14: R30, 2012.
35. Gandhi UH, Kaushal N, Ravindra KC, Hegde S, Nelson SM, Narayan V, Vunta H, Paulson RF and Prabhu KS: Selenoprotein-dependent up-regulation of hematopoietic prostaglandin D2 synthase in macrophages is mediated through the activation of peroxisome proliferator-activated receptor (PPAR) gamma. J Biol Chem 286: 27471-27482, 2011.
36. Okinaga T, Mohri I, Fujimura H, Imai K, Ono J, Urade Y and Taniike M: Induction of hematopoietic prostaglandin D synthase in hyalinated necrotic muscle fibers: Its implication in grouped necrosis. Acta Neuropathol 104: 377-384, 2002.
37. Mohri I, Aritake K, Taniguchi H, Sato Y, Kamauchi S, Nagata N, Maruyama T, Taniike M and Urade Y: Inhibition of prostaglandin D synthase suppresses muscular necrosis. Am J Pathol 174: 1735-1744, 2009.